Electronic Supplementary Information (ESI)

For

Cyclometalated Iridium(III) Complex of a 1,2,3-Triazole-based Ligand for Highly Selective Sensing of Pyrophosphate Ion

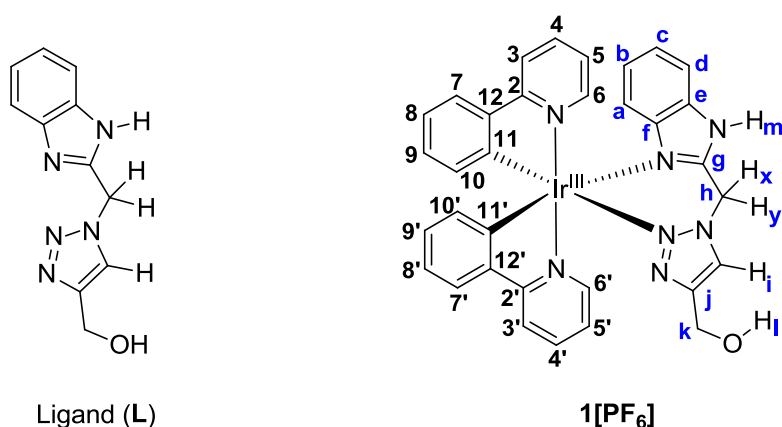Monosh Rabha,[a] Bhaskar Sen,[a] Sanjoy Kumar Sheet,[a] Kripamoy Aguan,[b] and Snehadrinarayan Khatua*[a]

*[a]Centre for Advanced Studies, Department of Chemistry, North-Eastern Hill University, Shillong, Meghalaya 793022, India. *Email: snehadri@gmail.com; skhatua@nehu.ac.in.*
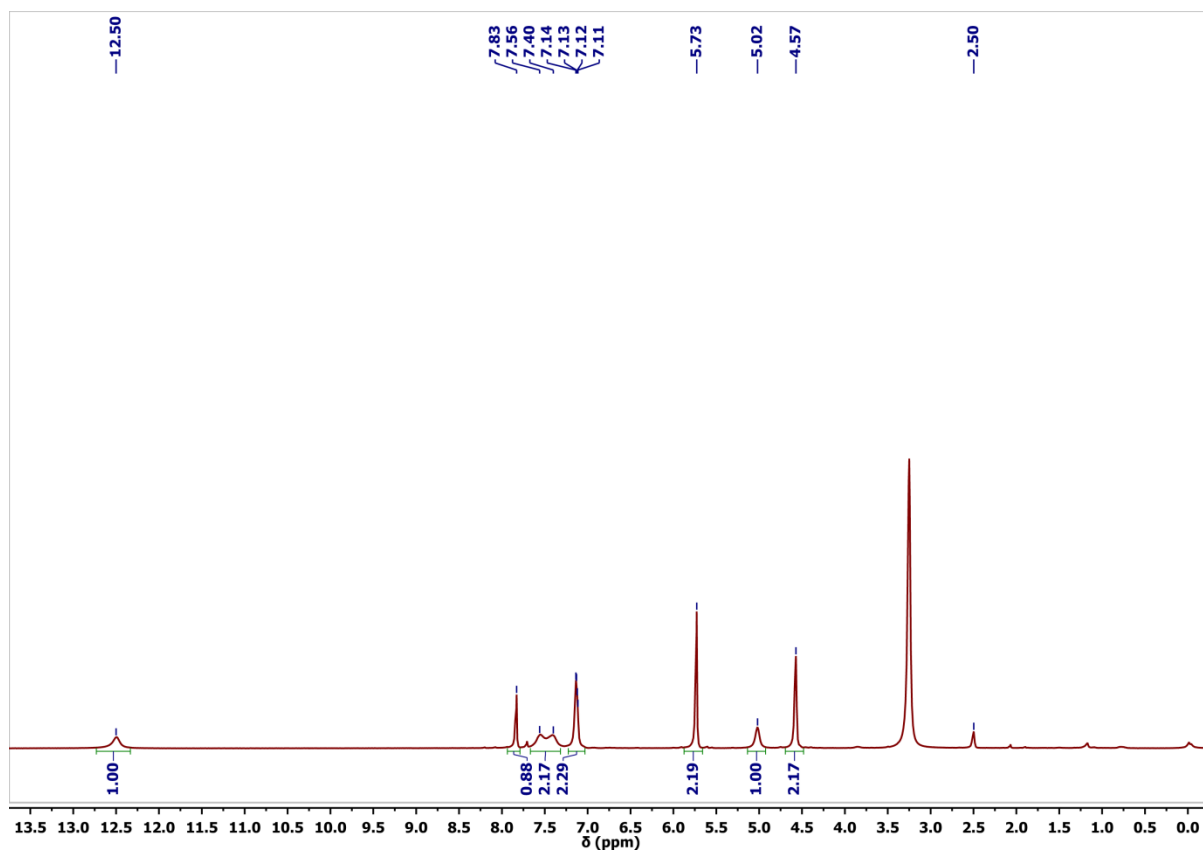*[b]Department of Biotechnology and Bioinformatics, North-Eastern Hill University, Shillong, Meghalaya 793022, India.*
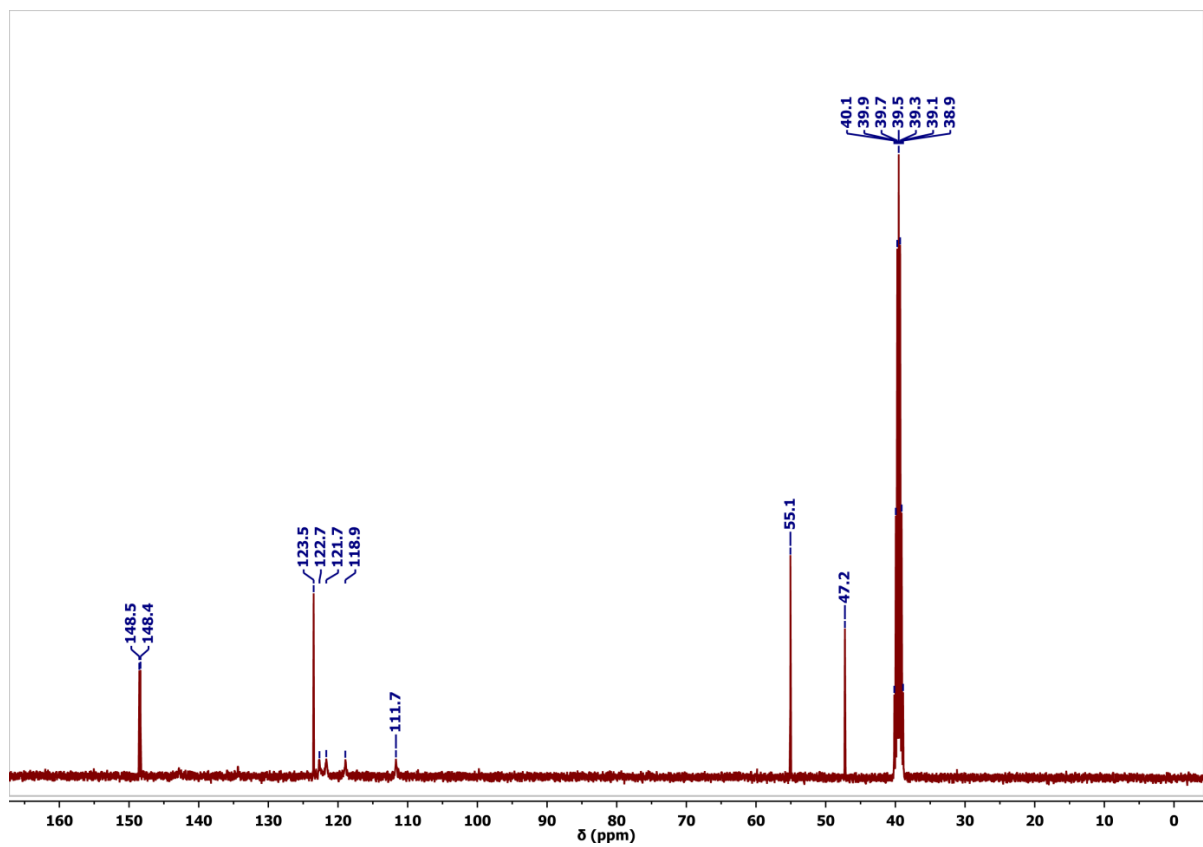
Table of Contents

Contents   Page no

Chart S1. List of Compounds used in this study.

Ligand (**L**)   **1[PF$_6$]**

Figure S1. ^{1}H NMR of ligand **L** in DMSO-d$_{6}$.

Figure S2. ^{13}C NMR of ligand **L** in DMSO-d$_{6}$.
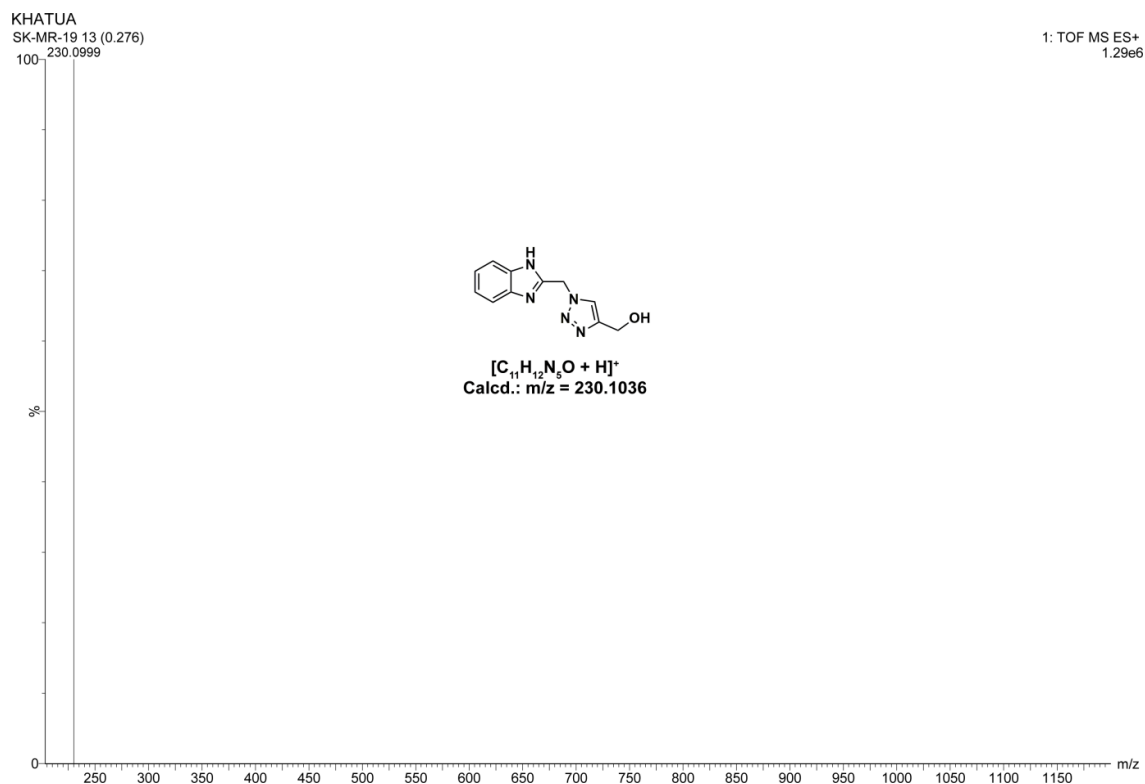
Figure S3. HRMS spectrum of ligand **L** in methanol.
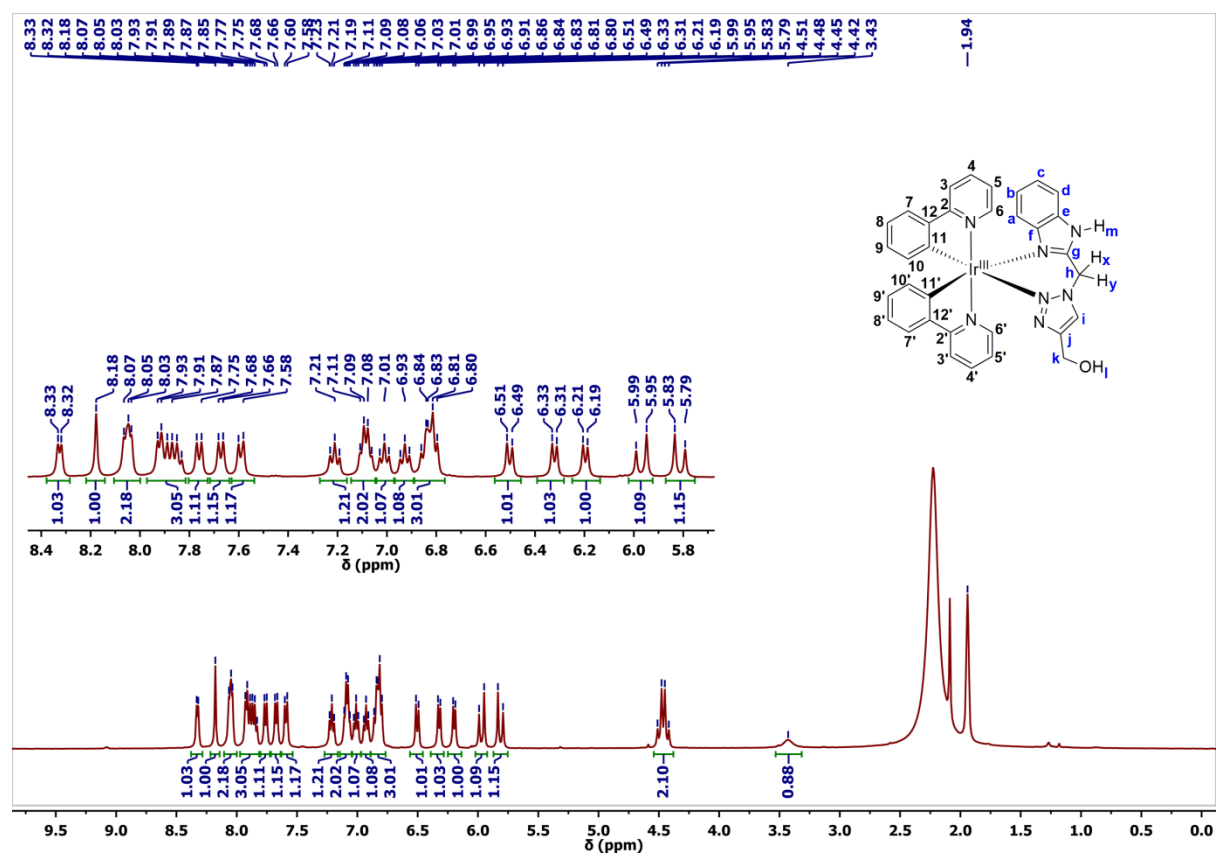
Figure S4. ^{1}H NMR of complex **1[PF$_6$]** in CD$_3$CN.
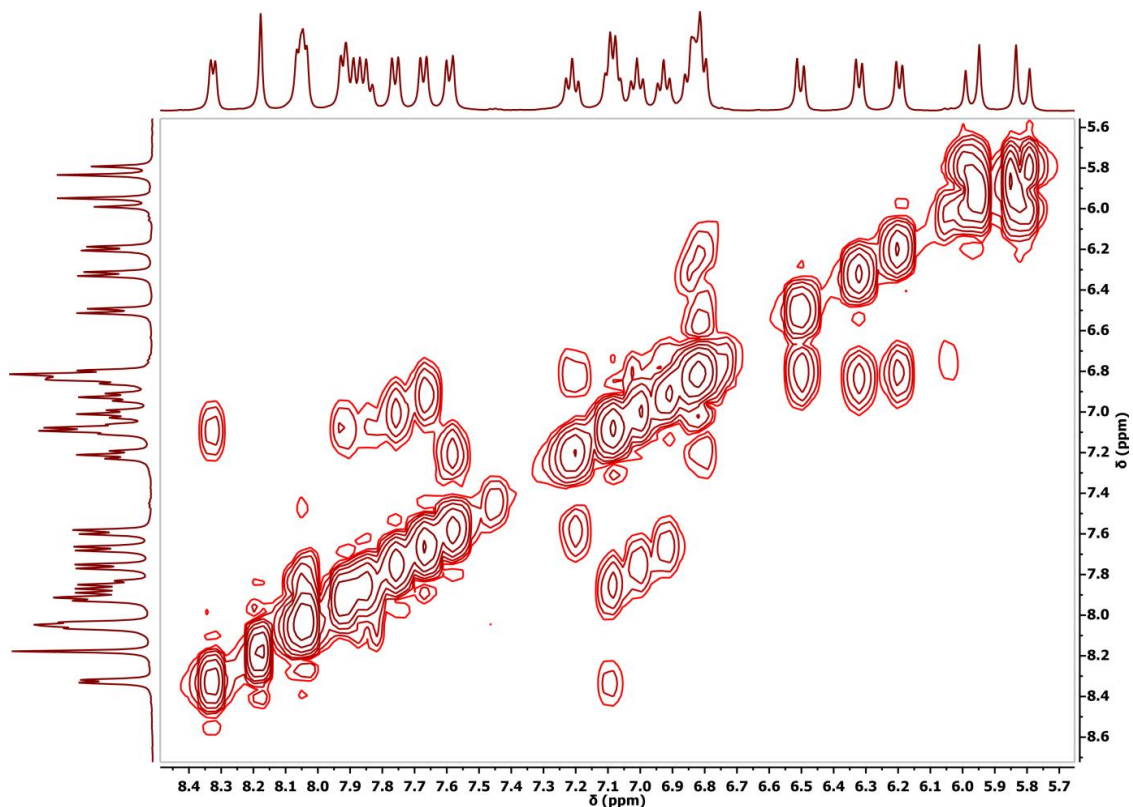
Figure S5. ^{1}H-^{1}H COSY NMR spectrum of **1[PF$_6$]** in CD$_3$CN.
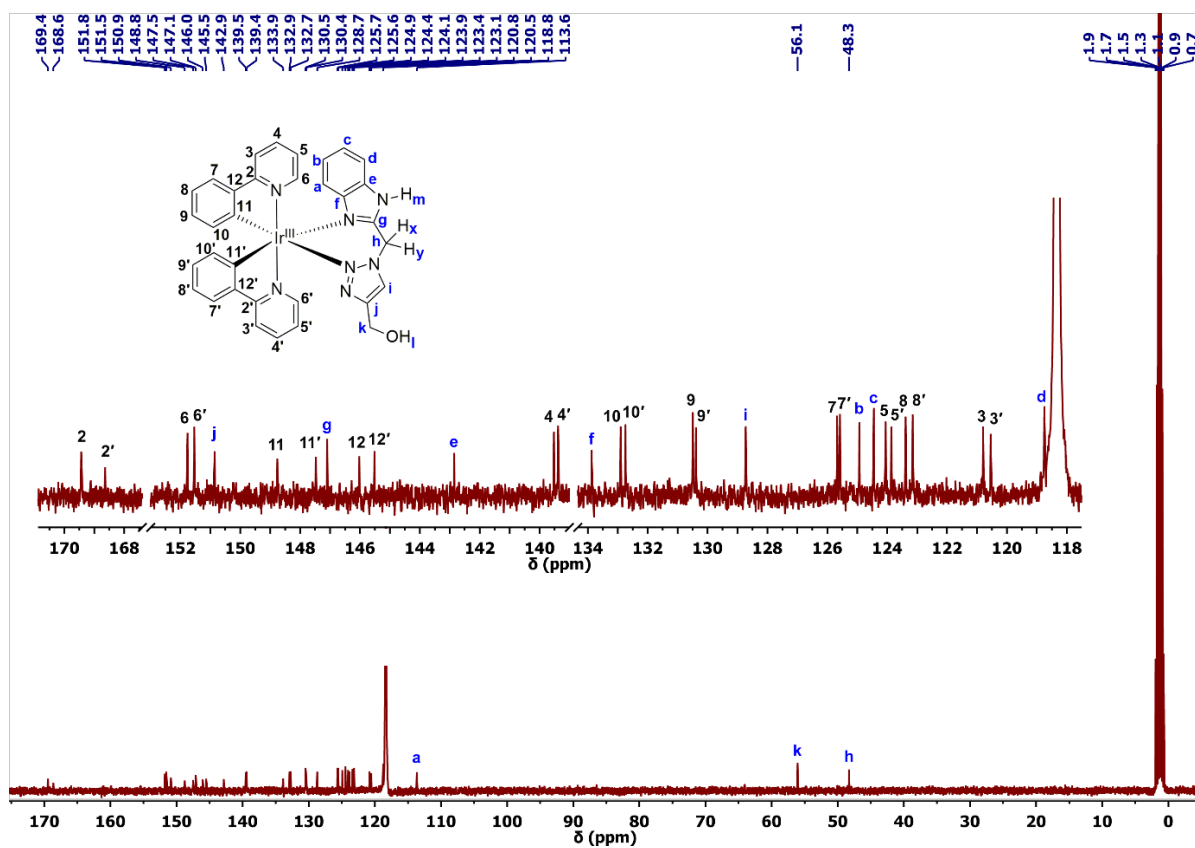
Figure S6. ^{13}C NMR spectrum of **1[PF$_6$]** in CD$_3$CN
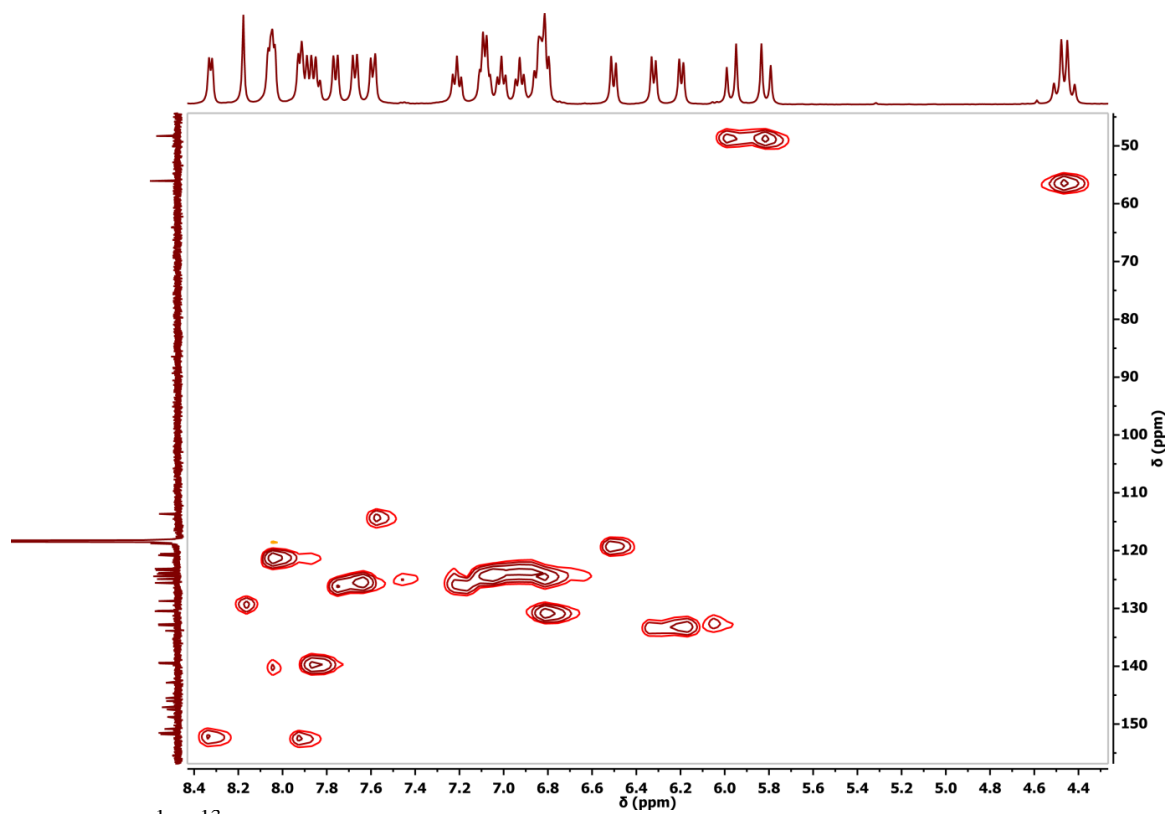
Figure S7. ^{1}H-^{13}C HSQC NMR spectrum of **1[PF$_6$]** in CD$_3$CN.
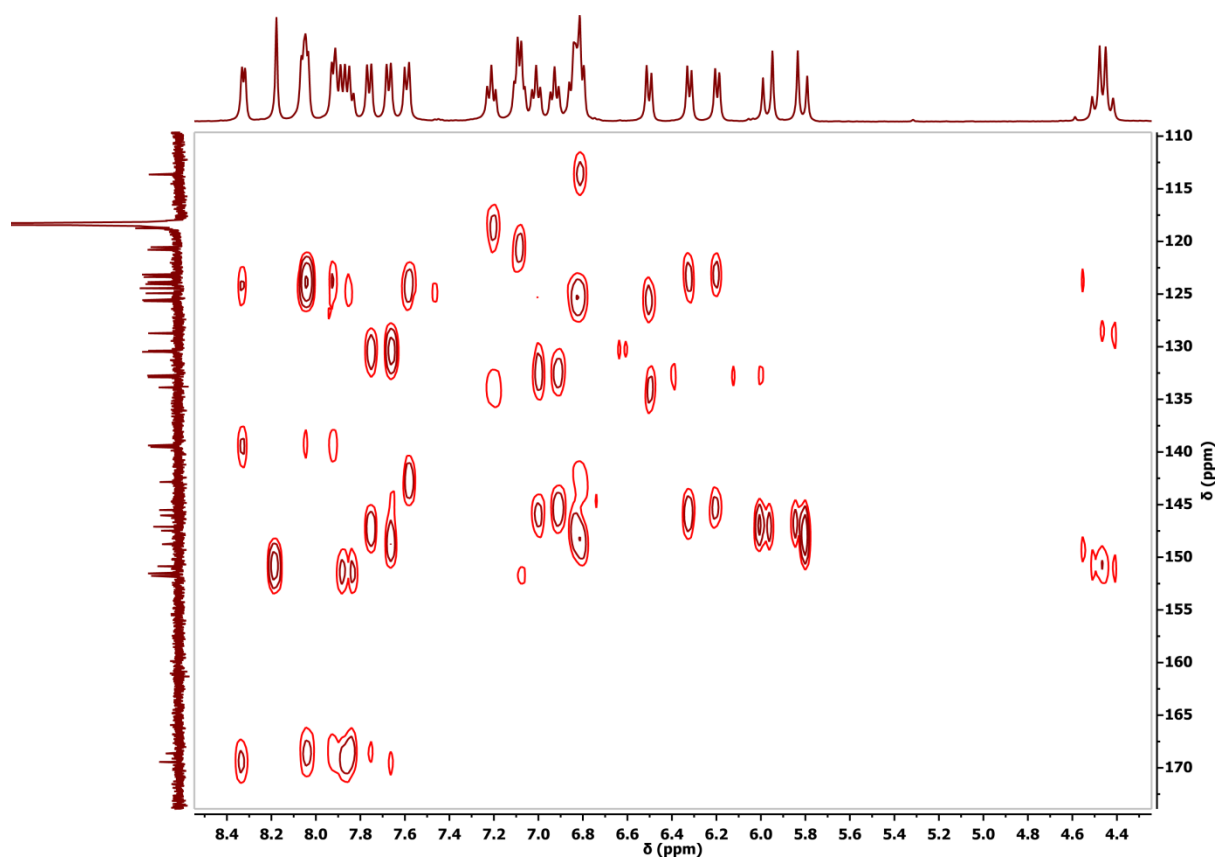
Figure S8. ^{1}H-^{13}C HMBC NMR spectrum of **1[PF$_6$]** in CD$_3$CN.
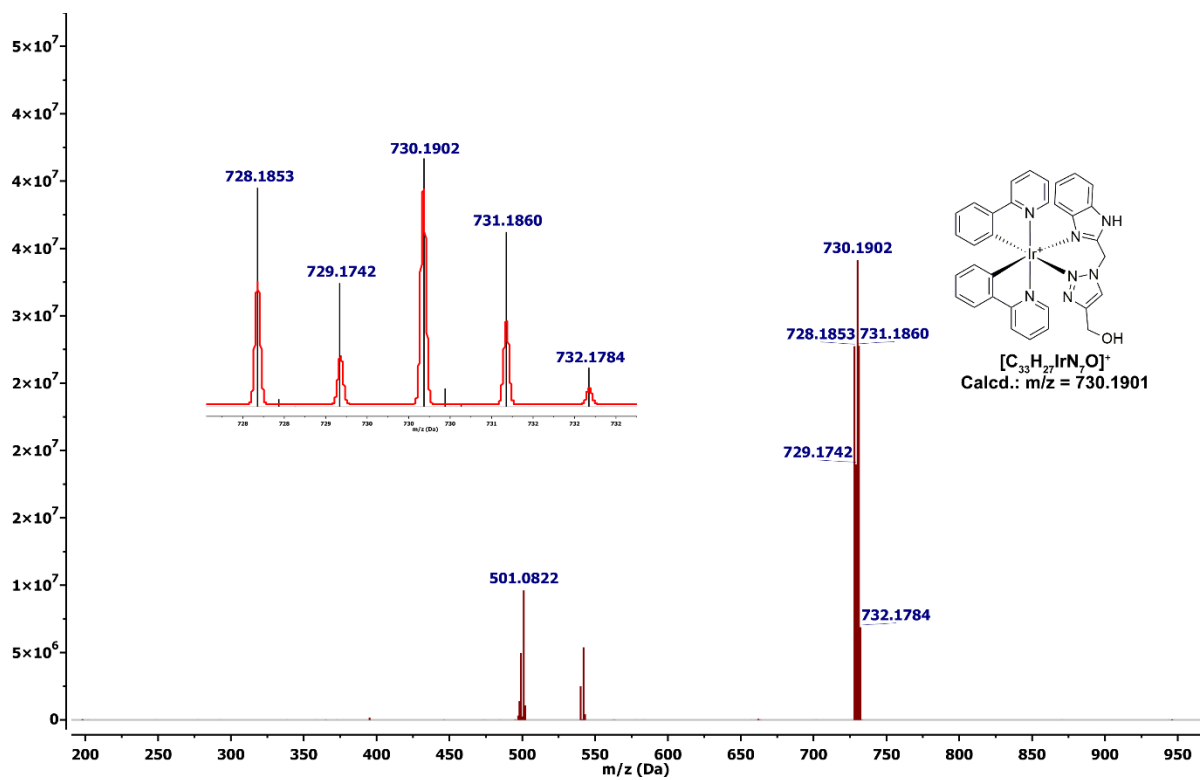
Figure S9. HRMS spectrum of **1[PF$_6$]** in CH$_3$CN.
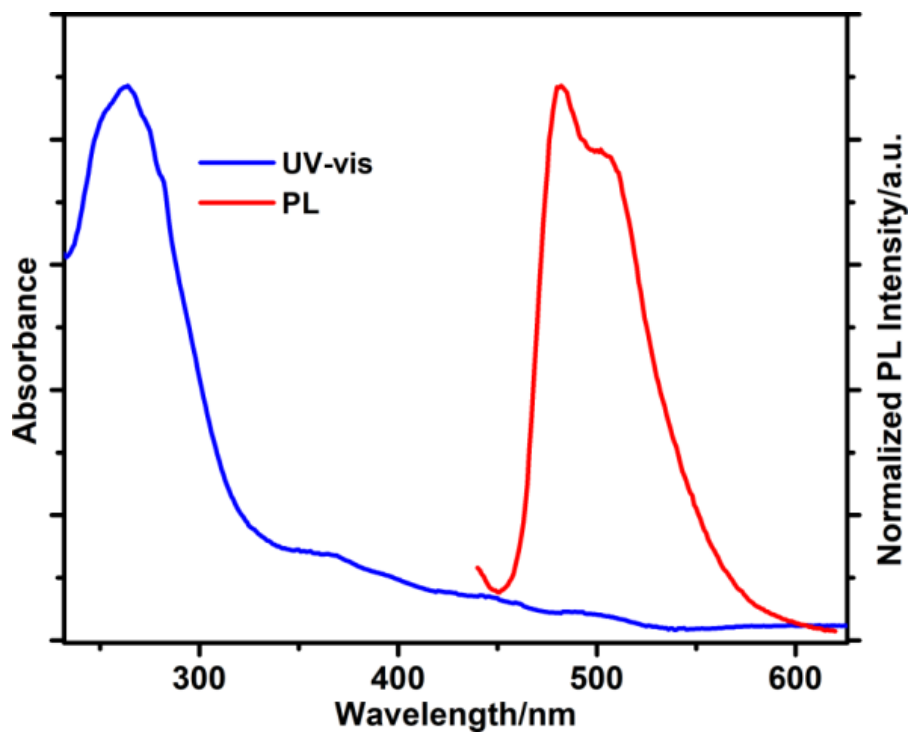
Figure S10. Normalized UV−vis and PL spectra of **1[PF$_6$]** in CH$_3$CN at room temperature.
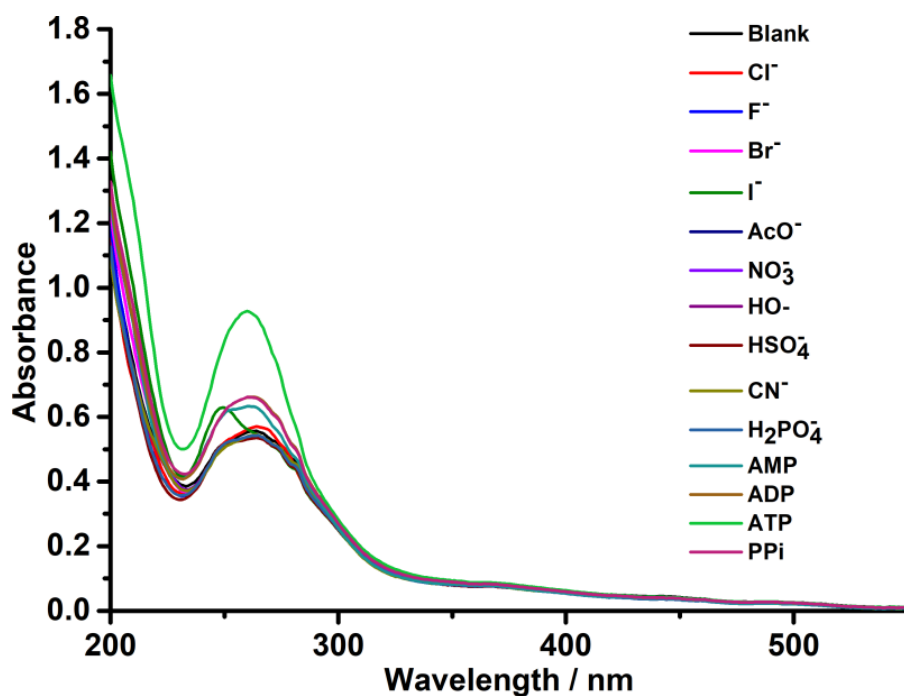
Figure S11. UV-vis selectivity of **1[PF$_6$]** (10 μM) in CH$_3$CN with various anions.
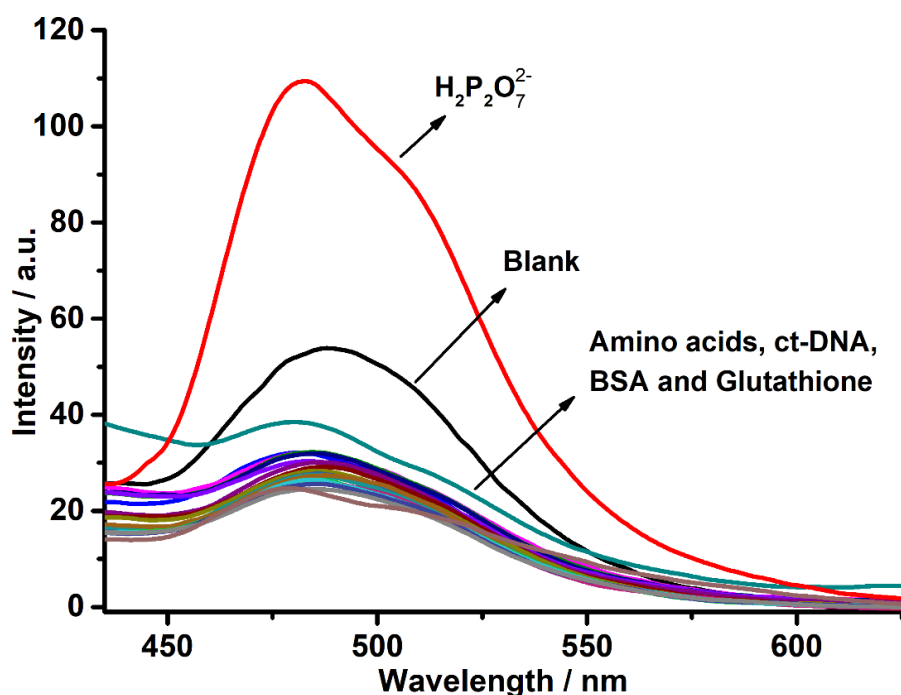
Figure S12. PL selectivity of **1[PF$_6$]** (10 μM) with amino acids (Isoleucine, Tyrosine, Alanine, Leucine, Arginine, Glutamic acid, Glycine, Proline, Serine, Tryptophan, Valine, Histidine, Aspartic acid, Phenylalanine), BSA protein, ct-DNA, Cysteine, Glutathione, and H$_2$P$_2$O$_7^{2-}$ (30 μM) in CH$_3$CN containing 1% HEPES buffer (0.01 M, pH 7.4) (λ_{ex} = 370 nm).
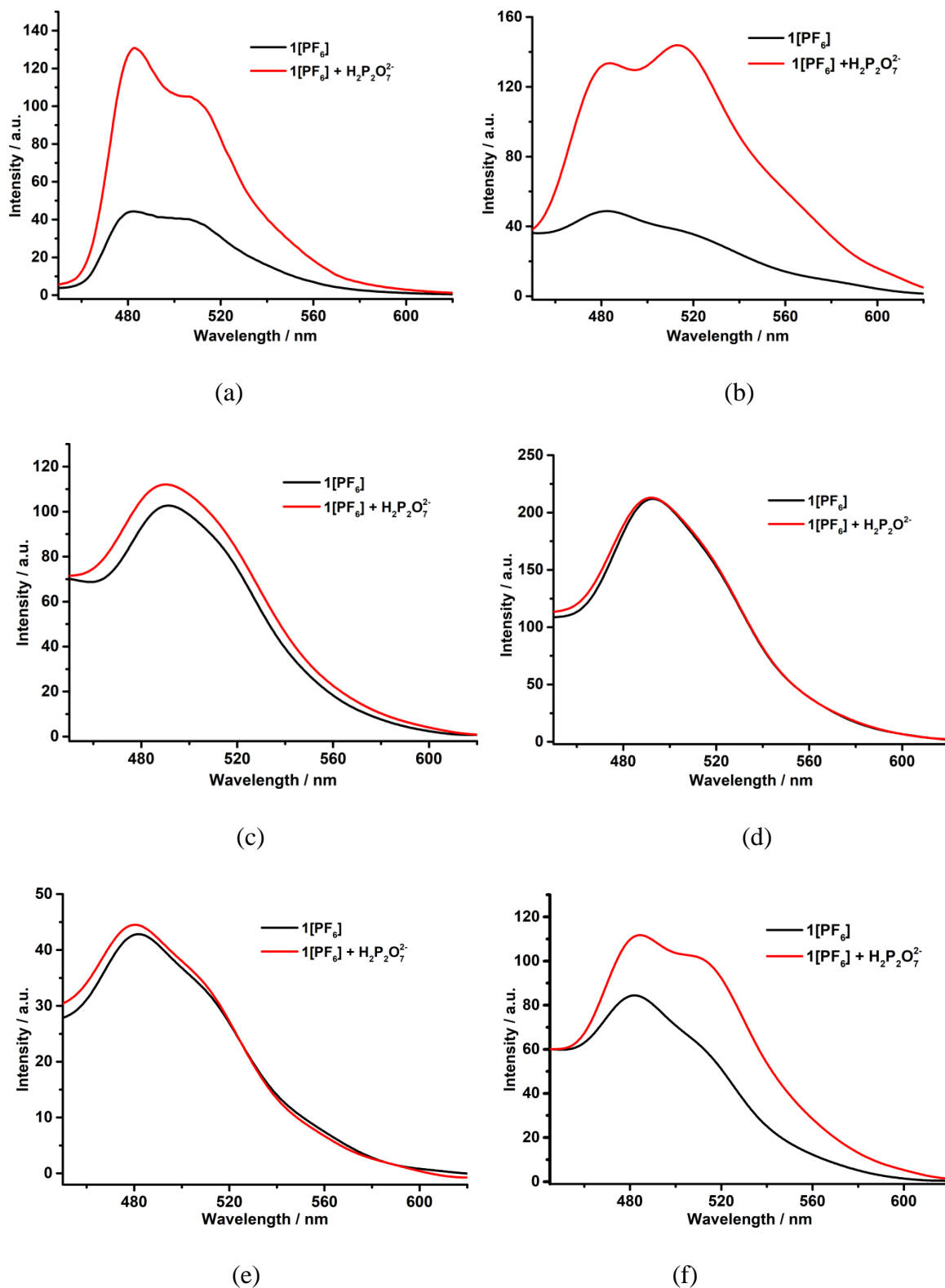
Figure S13. PL spectra of **1[PF$_6$]** (10 μM) and in the presence of **H$_2$P$_2$O$_7^{2-}$** (30 μM) in different solvents: (a) CH$_3$CN, (b) DCM, (c) DMF, (d) DMSO, (e) MeOH, and (f) THF (λ$_{ex}$ = 370 nm).

X-Ray Crystallography

Single crystals of **1[PF$_6$],** were obtained from a dichloromethane/methanol (1:1; v/v) solvent mixture. The X-ray data of **1[PF$_6$]** was collected at 293 K with Agilent Xcalibur (Eos, Gemini) diffractometer using graphite-monochromated Mo Kα radiation (λ = 0.71073 Å). For **1[PF$_6$]**, the data was collected, reduced, and cell refinement was done in CrysAlis PRO (Agilent, 2013) software.[1] The absorption was corrected by SCALE3 ABSPACK multi-scan method in CrysAlisPro. The structures of **1[PF$_6$]** was solved by direct methods using the program SHELXS-97[2] and refined by full-matrix least-squares calculations (F^2) by using the SHELXL-2018/3 software[3] within the WinGX[4] environment. All non-H atoms for **1[PF$_6$]**, were refined anisotropically against F^2 for all reflections. All hydrogen atoms except water hydrogen were placed at their calculated positions and refined isotropically. Unfortunately, it was not possible to collect complete good data set for **1[PF$_6$]** due to its poor quality. Attempt to refine all the non-H atoms anisotropically failed due to low-quality datasets, so all non-H atoms such as C22 and C33 for **1[PF$_6$]** were refined isotropically. There are six A-level alerts in the check cif file which are due to the high ADP N$_6$ atom, which is N.P.D. or nearly 2D. Several atoms, such as O$_1$, C$_{11}$, C$_{24}$, C$_{25}$, and C$_{27}$, had very high ADP**.** Several trials failed to refine to structure further. Crystal data collection and refinement details, selected bond lengths, and angles for **1[PF$_6$]** are given in Table S1 to Table S2 in ESI, respectively. The .cif file was deposited with the Cambridge Crystallographic Data Centre, and the following code was allocated: CCDC-2173561 for **1[PF$_6$]**.
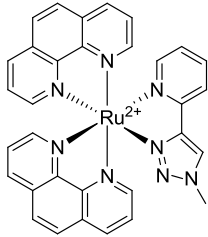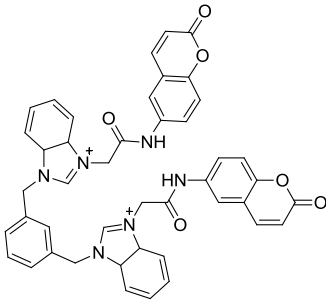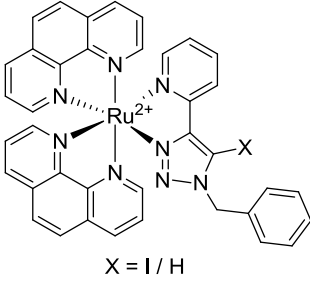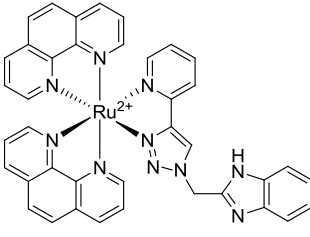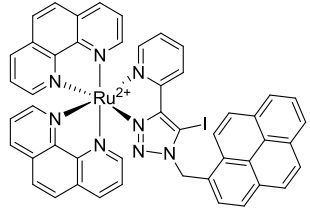
Table S1. Crystal data and structure refinement for **1[PF$_6$]**.
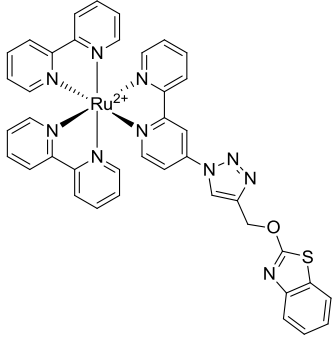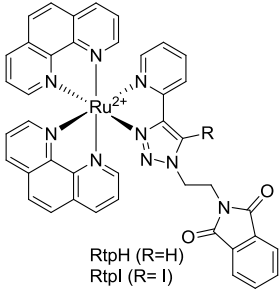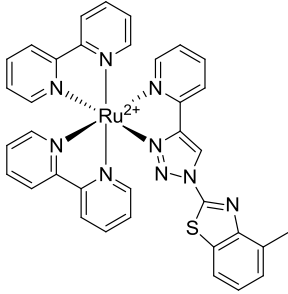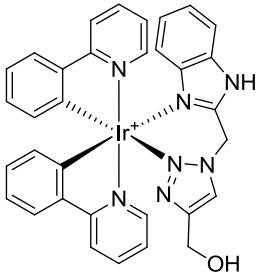
Empirical formula	$C_{33}H_{29}F_6IrN_7O_2P$
Formula weight	892.80
Temperature	293(2) K
Wavelength	0.71073 Å
Crystal system	Monoclinic
Space group	$P2_1/c$
Unit cell dimensions	$a = 15.508(3)$ Å $\quad \alpha = 90°.$
	$b = 13.606(4)$ Å $\quad \beta = 112.56(2)°.$
	$c = 18.951(3)$ Å $\quad \gamma = 90°.$
Volume	3692.4(16) Å^3
Z	4
Density (calculated)	1.606 Mg/m^3
Absorption coefficient	3.729 mm^{-1}
F(000)	1752
Crystal size	0.140 x 0.100 x 0.070 mm^3
Theta range for data collection	3.267 to 29.093°.
Index ranges	-20<=h<=19, -17<=k<=15, -24<=l<=25
Reflections collected	13635
Independent reflections	8371 [R(int) = 0.1194]
Completeness to theta = 26.000°	99.0 %
Absorption correction	Semi-empirical from equivalents
Max. and min. transmission	0.914 and 0.854
Refinement method	Full-matrix least-squares on F^2
Data / restraints / parameters	8371 / 12 / 443
Goodness-of-fit on F^2	1.060
Final R indices [I>2sigma(I)]	$R1 = 0.1312$, $wR2 = 0.3105$
R indices (all data)	$R1 = 0.2274$, $wR2 = 0.3778$

Table S2. Selected bond lengths [Å] and angles [°] for **1[PF₆]**.

Bond Length [Å]			
N(7)-Ir(1)	1.98(2)	C(22)-Ir(1)	2.007(18)
C(33)-Ir(1)	2.077(19)	N(1)-Ir(1)	2.174(15)
N(2)-N(4)	1.31(2)	N(2)-Ir(1)	2.217(15)
N(6)-Ir(1)	2.00(2)		

Bond Angles [°]			
N(7)-Ir(1)-N(6)	175.0(7)	N(7)-Ir(1)-C(22)	95.8(6)
N(6)-Ir(1)-C(22)	81.9(6)	N(7)-Ir(1)-C(33)	82.1(8)
N(6)-Ir(1)-C(33)	93.3(8)	C(22)-Ir(1)-C(33)	88.1(7)
N(7)-Ir(1)-N(1)	86.7(6)	N(6)-Ir(1)-N(1)	95.8(7)
C(22)-Ir(1)-N(1)	175.9(6)	C(33)-Ir(1)-N(1)	95.5(7)
N(7)-Ir(1)-N(2)	95.4(7)	N(6)-Ir(1)-N(2)	89.1(7)
C(22)-Ir(1)-N(2)	90.0(6)	C(33)-Ir(1)-N(2)	176.7(7)
N(1)-Ir(1)-N(2)	86.5(6)		

Table S3. Comparison of **1[PF₆]** with other chemosensors for luminescent pyrophosphate detection.

Sl. No.	Probe	LOD of pyrophosphate	Analytes	Reference
1		0.45 µM	PPi & $H_2PO_4^-$	*Inorg. Chem.* **2014**, *53*, 806−8070.
2		2.59 µM	PPi & $H_2PO_4^-$	*RSC Adv.* **2015**, *5*, 46608–46616.
3		0.09 µM (I) and 0.25 µM (H)	PPi & $H_2PO_4^-$	*Chem. Eur. J.* **2016**, *22*, 18051–18059.
4		0.03 µM	PPi & $H_2PO_4^-$	*Inorg. Chem.* **2017**, *56*, 1249−263.
5		0.41 µM	PPi & $H_2PO_4^-$	*Inorg. Chem.* **2019**, *58*, 15993−16003.

6		0.31 μM	PPi & $H_2PO_4^-$	*New J. Chem.* **2020**, *44*, 6186–6196.
7	 RtpH (R=H) RtpI (R= I)	0.202 μM (RtpH) & 0.177 μM (RtpI)	PPi & $H_2PO_4^-$	*Analyst*, **2021**, *146*, 1430–1443.
8		0.43 μM	PPi & $H_2PO_4^-$	*Eur. J. Inorg. Chem.* **2021**, 3549–3560.
9		127 nM	Pyrophosphate ($H_2P_2O_7^{2-}$)	*Present Work*
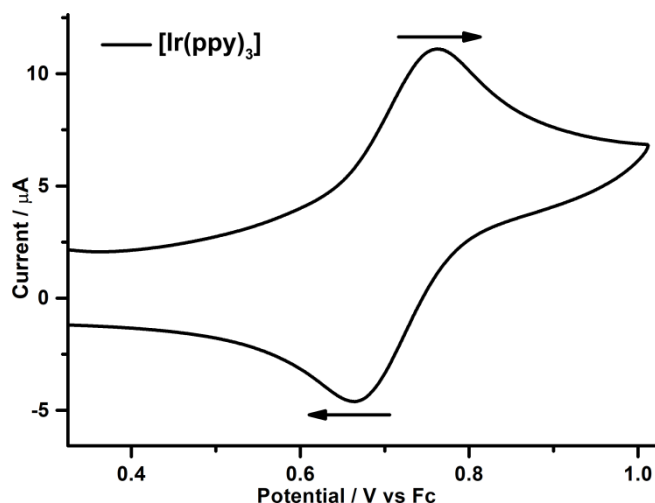
Figure S14. Cyclic voltammetric (CV) of 1.0 mM **[Ir(ppy)₃]** in dry and degassed acetonitrile in the presence of 0.1 M tetra-n-butylammonium perchlorate (Bu_4NClO_4) as a supporting electrolyte and potential axis was calibrated with Ferrocene.

DFT Calculations

The geometry optimization for the free complex **1**, the pyrophosphate adduct, **1•$H_2P_2O_7^{2-}$** were performed using DFT in the ground state. After the interaction between **1** and **$H_2P_2O_7^{2-}$** –174.51 Kcal/mol free energy is released (Figure S15) due to the formation of **1•$H_2P_2O_7^{2-}$** adduct through long chain H-bonding interaction between compound **1** and oxygen atoms of **$H_2P_2O_7^{2-}$**.
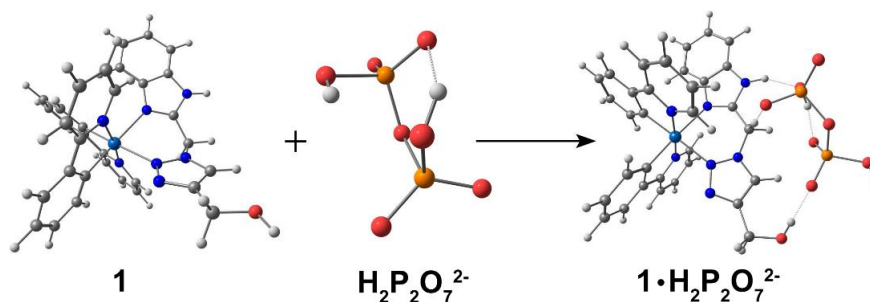
Figure S15. The optimized structures of complex **1**, **$H_2P_2O_7^{2-}$**, and **1•$H_2P_2O_7^{2-}$** in the ground state show the H-bonding interaction between host and guest.

Calculation of stabilization energy for 1•$H_2P_2O_7^{2-}$.

E_1 = −1152656.08 kcal/mol; $E_{H_2P_2O_7^{2-}}$ = −759706.37 kcal/mol; $E_{1•H_2P_2O_7^{2-}}$ = −1912536.96 kcal/mol

$\Delta E = E_{1•H_2P_2O_7^{2-}} - (E_1 + E_{H_2P_2O_7^{2-}})$

$= -1912536.96 - \{-1152656.08 + (-759706.37)\}$ kcal/mol

$= -174.51$ kcal/mol.

The singlet state TDDFT calculations on the ground state optimized geometry of **1** and **1•H₂P₂O₇²⁻** were performed to assign the MLCT and/or LLCT transitions responsible for the corresponding absorption spectra in acetonitrile. The involved molecular orbitals (MOs) with transition energies between the low-lying HOMOs and LUMOs of **1** and **1• H₂P₂O₇²⁻** obtained from the theoretical calculation are shown in Figure S16, and their associated oscillator strengths are represented in Table S4, where HOMO of both **1** exhibits the dx^2-y^2(Ir) orbital of metal and π orbitals of ancillary 2-phenylpyridine and analyte target benzimidazole-triazole ligands. On the other hand, the LUMO of **1** is mainly distributed on the dz^2(Ir) and 2-phenylpyridine parts of ligand **L**. The estimated value for the HOMO – LUMO energy gap from the DFT calculation for complex **1** is calculated to be 3.86 eV, respectively. The TDDFT-based calculated vertical excitation energies, corresponding oscillator strengths (f) and compositions of the related transitions assigned to the experimental UV-vis spectrum in CH₃CN are displayed in Table S4. The TDDFT calculations indicate that the experimentally obtained spin-allowed π–π* transition band at λ_{max} = 263 nm (4.71 eV) of **1** is due to the strong transitions from HOMO → LUMO + 6, HOMO − 4 → LUMO + 2 and HOMO − 7 → LUMO + 1 (f = 0.019) (265 nm, 4.67 eV). The shoulder at longer wavelengths in the region of 355 to 435 nm with λ_{max} = 370 nm was characterized as HOMO → LUMO + 2 (f = 0.025) (340 nm, 3.64 eV) and HOMO → LUMO + 1 (f = 0.021) (386 nm, 3.21 eV).
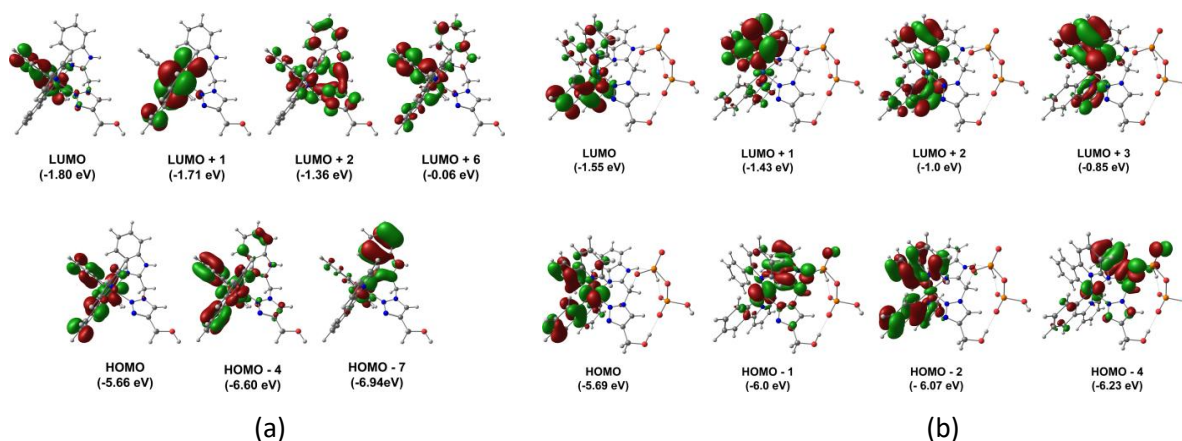
Figure S16. Representative plots of molecular orbitals (MOs) of (a) compound **1**, (b) **1•H₂P₂O₇²⁻** obtained from singlet state TDDFT calculation at the ground state optimized geometry in CH₃CN [isovalue = 0.03].

Table S4: Selected singlet state electronic transitions obtained from TDDFT calculation at B3LYP/6-31G (d) // LANL2DZ level of **1** and **1• $H_2P_2O_7^{2-}$** in CH_3CN.

Complex	Experimentally observed transition (nm) / eV	Computed vertical excitation energy (nm) / eV	Composition	Oscillator strength (*f*)	Contribution (CI)
1	263 nm (4.71 eV)	264 nm (4.68 eV)	HOMO – 7 → LUMO + 1	0.115	0.28
			HOMO – 4 → LUMO + 2		0.32
			HOMO → LUMO + 6		0.28
	370 nm (3.35 eV)	340 nm (3.64 eV)	HOMO → LUMO + 2	0.025	0.68
		386 nm (3.21 eV)	HOMO → LUMO + 1	0.021	0.69
1• $H_2P_2O_7^{2-}$	261 nm (4.75 eV)	263 nm (4.70 eV)	HOMO – 4 → LUMO + 2	0.126	0.46
		268 nm (4.62 eV)	HOMO – 2 → LUMO + 3	0.158	0.40
	370 nm (3.35 eV)	322 nm (3.85 eV)	HOMO – 1 → LUMO + 1	0.109	0.44
		377 nm (3.28 eV)	HOMO – 1 → LUMO	0.009	0.60

Table S5. The x,y,z Cartesian coordinates of the complex **1**, and **1•H$_2$P$_2$O$_7$$^{2-}$** obtained from DFT optimization at B3LYP/6-31G (d) // LANL2DZ level.

Complex **1**

	X	Y	Z		X	Y	Z
C	-0.58026	-5.02969	-0.70568	N	-2.62449	0.63665	-0.40818
C	-0.3156	-4.67675	0.59005	N	-1.83013	-0.29943	0.25941
C	-0.0578	-3.19631	0.95265	N	-2.49076	-1.09966	0.95945
C	-0.10591	-2.28665	-0.03978	C	-3.89779	-0.93507	0.56775
C	-0.34531	-2.67461	-1.47512	C	-3.95029	0.03084	-0.35299
C	-0.59619	-3.95466	-1.81905	C	-5.09246	-1.74191	1.10933
C	2.91789	-0.75056	-1.27602	O	-6.09704	-1.84409	0.09679
C	4.26758	-0.91399	-1.23094	H	-0.775	-6.05302	-0.95016
C	5.01263	-0.88099	0.12554	H	-0.28876	-5.42627	1.3532
C	4.31984	-0.68566	1.27718	H	0.14846	-2.90291	1.96078
C	2.79821	-0.49926	1.20404	H	-0.79709	-4.22046	-2.83582
C	2.14289	-0.53046	0.03295	H	2.40118	-0.77547	-2.21267
C	-0.24653	-1.46697	-2.43649	H	4.81639	-1.06634	-2.13673
C	1.89463	-0.26721	2.40112	H	6.07414	-1.01204	0.15584
N	0.02863	-0.30896	-1.87286	H	4.82625	-0.66169	2.21943
C	0.26016	0.90006	-2.68086	H	0.52326	1.821	-2.20383
C	0.13376	0.84583	-4.03378	H	0.29904	1.72345	-4.62314
C	-0.25122	-0.48222	-4.71678	H	-0.37259	-0.53026	-5.77881
C	-0.43038	-1.58617	-3.95605	H	-0.69024	-2.52261	-4.40377
C	2.30877	-0.21059	3.68486	H	3.33529	-0.37218	3.93993
C	1.26377	0.09734	4.76853	H	1.54688	0.15113	5.79901
C	-0.02448	0.30206	4.394	H	-0.76866	0.53306	5.12728
C	-0.40917	0.19745	2.90117	H	-1.42163	0.35724	2.59418
N	0.50076	-0.08895	2.02284	H	3.55203	5.57771	-0.73282
Ir	0.11025	-0.2951	0.101	H	4.4592	3.11587	-0.73562
C	2.89071	4.76623	-0.5113	H	2.93185	1.24812	-0.31012
C	3.42599	3.30282	-0.52954	H	1.20545	6.01908	-0.18831
C	2.58161	2.25893	-0.28875	H	-1.30169	4.46556	0.03443
C	1.11487	2.58164	0.00317	H	-3.19906	2.61982	-0.08169
C	0.67867	3.825	0.10523	H	-2.86425	1.69364	1.36118
C	1.58374	5.0184	-0.21009	H	-4.80095	0.30434	-0.94162
N	-0.01195	1.66973	0.17985	H	-4.76457	-2.72197	1.38662
C	-1.09494	2.40223	0.35479	H	-5.4987	-1.24603	1.96603
N	-0.72379	3.82808	0.54401	H	-6.8418	-2.34697	0.43454
C	-2.55552	1.88474	0.35468				

1•H₂P₂O₇²⁻

	X	Y	Z		X	Y	Z
C	-1.11117	-5.54362	2.72229	C	-0.41217	-3.81329	-1.49646
C	0.19868	-5.11249	2.74618	Ir	-0.27745	-1.0926	1.15307
C	0.53763	-3.72407	2.20035	H	-0.54921	1.65929	-0.80827
C	-0.46761	-2.98448	1.74451	H	1.32555	1.30167	-1.30625
C	-1.87474	-3.45653	1.676	H	0.17055	3.33815	-0.485
C	-2.2273	-4.64527	2.12922	O	-0.02049	1.32813	-4.67681
C	-2.79692	-2.43078	1.06644	P	-0.83928	2.37995	-3.66296
N	-2.21565	-1.31917	0.71978	O	-2.17429	1.60046	-3.31354
C	-3.00519	-0.24843	0.03844	O	-1.28191	4.01132	-3.87789
C	-4.35582	-0.41623	-0.17223	O	0.2181	2.51868	-2.44311
C	-5.05189	-1.70744	0.28646	P	-1.36955	4.12329	-2.10209
C	-4.30127	-2.67187	0.87533	O	-2.21923	5.35526	-1.33207
C	4.4438	-0.698	1.81208	O	-2.00004	2.8822	-1.65403
C	4.0379	-1.02052	0.55154	O	0.20878	4.25924	-1.48482
C	2.5181	-1.16507	0.25509	H	-0.44487	0.317	-3.57991
N	1.67841	-0.99798	1.23628	H	-1.65546	5.39289	0.08292
C	2.113	-0.65981	2.58381	H	0.65652	3.28343	-2.73997
C	3.38874	-0.49572	2.90833	H	-3.14661	5.16055	-1.26585
C	0.9583	-0.47449	3.57788	H	-1.35736	-6.49753	3.111
C	-0.24277	-0.64292	3.06914	H	0.9764	-5.71751	3.13319
C	-1.53521	-0.44657	3.84875	H	1.52567	-3.33379	2.19107
C	-1.43147	-0.11462	5.14922	H	-3.24975	-4.9649	2.08828
C	-0.01591	0.07591	5.78699	H	-2.52877	0.66106	-0.28268
C	1.11168	-0.08553	5.03408	H	-4.92535	0.35234	-0.65894
C	-0.15388	-0.12426	-1.46082	H	-6.10453	-1.85973	0.14953
C	0.31174	1.23243	-0.96884	H	-4.7482	-3.59136	1.20418
N	0.4555	1.43996	0.39933	H	5.47848	-0.59707	2.05176
C	-0.15738	2.72196	0.33604	H	4.75795	-1.15722	-0.23459
C	-1.04301	2.87524	1.29458	H	2.16885	-1.37302	-0.7379
N	-1.11607	1.54194	1.94805	H	3.65634	-0.23102	3.90981
N	-0.37809	0.79454	1.22722	H	-2.48767	-0.55279	3.36947
C	-1.82629	4.188	1.60049	H	-2.31258	0.03028	5.72545
O	-1.24936	5.36146	0.9575	H	0.06695	0.33084	6.81506
N	-0.7211	-0.34109	-2.866	H	2.0822	0.05323	5.45282
C	-0.42046	-1.77684	-2.9729	H	-1.81576	4.28895	2.64742
C	-0.342	-2.2999	-1.73153	H	-2.82753	4.13895	1.23031
N	-0.21947	-1.18766	-0.78036	H	-0.15609	-2.2033	-5.20194
C	-0.28011	-2.64368	-4.21738	H	-0.35521	-4.64606	-4.886
C	-0.36758	-4.00259	-4.03188	H	-0.60057	-5.68856	-2.4745
C	-0.47787	-4.61957	-2.59677	H	-0.41164	-4.22685	-0.50936

References

1. CrysAlisPro Software System, 1.171.36.28; Agilent Technologies UK Ltd.: Oxford, UK, **2013**.

2. G. M. Sheldrick, A short history of SHELX, *Acta Cryst.* **2008**, *A64*, 112-122.

3. (a) G. M. Sheldrick, SHELXL-97: Program for Crystal Structure Refinement; University of Gottingen: Gottingen, Germany, **1997**. (b) G. M. Sheldrick, SHELXT - Integrated space-group and crystal-structure determination, *Acta Cryst.* **2015**, *C71*, 3–8.

4. (a) L. J. Farrugia, WinGX suite for small-molecule single-crystal crystallography, *J. Appl. Cryst.* **1999**, *32*, 837–838. (b) L. J. Farrugia, WinGX and ORTEP for Windows: an update, *J. Appl. Cryst.* **2012**, *45*, 849–854.